The nuclear pore proteins Nup88/214 and T-cell acute lymphatic leukemia–associated NUP214 fusion proteins regulate Notch signaling

Bastian Kindermann[‡], Christina Valkova[‡], Andreas Krämer[‡], Birgit Perner[‡], Christian Engelmann[‡], Laura Behrendt[‡], Daniel Kritsch[§], Berit Jungnickel[§], ⬤ Ralph H. Kehlenbach[¶], Franz Oswald[‖], Christoph Englert[‡§], and ⬤ Christoph Kaether[‡1]

From the [‡]Leibniz Institut für Alternsforschung-Fritz Lipmann Institut, 07745 Jena, Germany, the [§]Institut für Biochemie und Biophysik, Friedrich Schiller Universität Jena, 07745 Jena, Germany, the [¶]Department of Molecular Biology, Universitätsmedizin Göttingen, 37073 Göttingen, Germany, and the [‖]Universitätsklinikum Ulm, Zentrum für Innere Medizin, Abteilung für Innere Medizin I, 89081 Ulm, Germany

Edited by Peter Cresswell

The Notch receptor is a key mediator of developmental programs and cell-fate decisions. Imbalanced Notch signaling leads to developmental disorders and cancer. To fully characterize the Notch signaling pathway and exploit it in novel therapeutic interventions, a comprehensive view on the regulation and requirements of Notch signaling is needed. Notch is regulated at different levels, ranging from ligand binding, stability to endocytosis. Using an array of different techniques, including reporter gene assays, immunocytochemistry, and ChIP-qPCR we show here, to the best of our knowledge for the first time, regulation of Notch signaling at the level of the nuclear pore. We found that the nuclear pore protein Nup214 (nucleoporin 214) and its interaction partner Nup88 negatively regulate Notch signaling _in vitro_ and _in vivo_ in zebrafish. In mammalian cells, loss of Nup88/214 inhibited nuclear export of recombination signal-binding protein for immunoglobulin κJ region (RBP-J), the DNA-binding component of the Notch pathway. This inhibition increased binding of RBP-J to its cognate promoter regions, resulting in increased downstream Notch signaling. Interestingly, we also found that NUP214 fusion proteins, causative for certain cases of T-cell acute lymphatic leukemia, potentially contribute to tumorigenesis via a Notch-dependent mechanism. In summary, the nuclear pore components Nup88/214 suppress Notch signaling _in vitro_, and in zebrafish, nuclear RBP-J levels are rate-limiting factors for Notch signaling in mammalian cells, and regulation of nucleocytoplasmic transport of RBP-J may contribute to fine-tuning Notch activity in cells.

Notch is required for cell–cell communication and regulates cell fate (1–3). Notch undergoes three proteolytic cleavage events, first by Furin (4), then, after ligand-binding, by ADAM/TACE (5); and finally by γ-secretase (6). γ-Secretase releases the Notch intracellular domain (NICD),[2] which is imported into the nucleus. There, it interacts with the DNA-binding protein RBP-J, also called CSL, and Mastermind proteins to control gene expression (7, 8). To fine-tune and control Notch signaling, a tight network of Notch activity control instances has evolved. Notch signal modulation can include acetylation (9), glycosylation (10), methylation (11), or ubiquitination (12–16) of the receptor. NICD activity can be regulated via phosphorylation by several kinases (17–20). Apart from post-translational modifications, the cleavage of Notch may also be regulated (21, 22).

Nucleocytoplasmic transport is mediated by exportins and importins that shuttle proteins through the nuclear pore (23, 24). Nuclear pore protein (Nup, or NUP in case of humans; we use Nup throughout the text for mammalian Nup and nup for zebrafish Nup) 214 is a peripheral FG-repeat Nup and is located on the cytoplasmic face of the nuclear pore. Together with its binding partner Nup88, Nup214 was shown to be involved in nuclear import and export (25–28). Interestingly, Nup214 fusion proteins were found in ~10% of T-cell acute lymphatic leukemia (T-ALL) cases, a fatal leukemia that is strongly associated with aberrant Notch signaling (29, 30).

We here identified Nup88 and Nup214 as novel negative regulators of Notch signaling _in vitro_ and _in vivo_. Nup88/214 negatively regulates the Notch co-factor RBP-J by decreasing its nuclear levels, thus reducing NICD-dependent transcription. T-ALL–associated Nup214 fusion proteins phenocopied a loss of Nup214 and up-regulated Notch, potentially contributing to tumorigenesis.
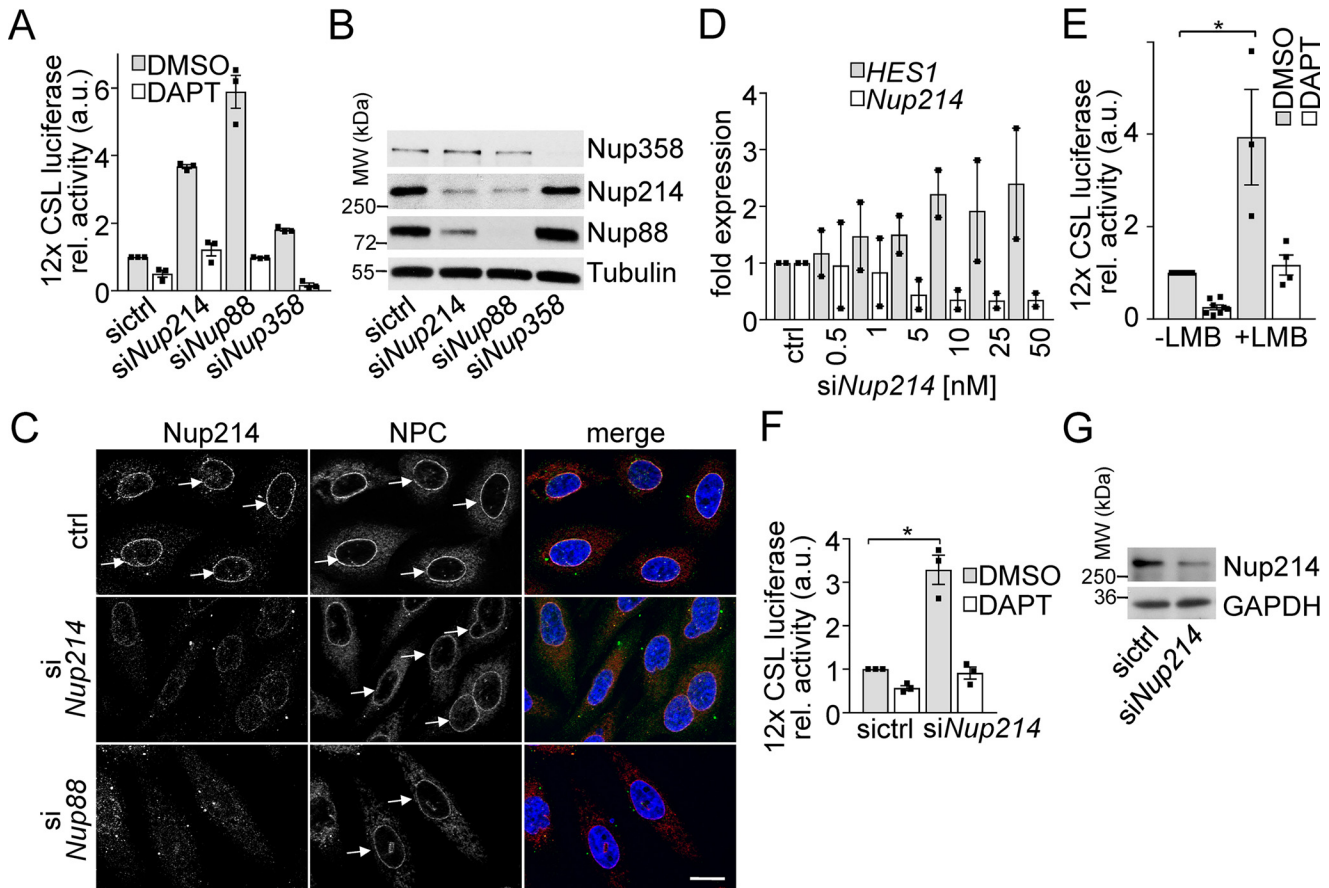
Figure 1. Nup88 and Nup214 negatively regulate canonical Notch signaling. *A–C*, PC3 cells were transfected with 12× CSL luciferase Notch reporter and siRNAs as indicated. 24 h later cells were harvested and subjected to luciferase assay (*A*) or probed with the indicated antibodies for protein expression (*B*) and immunofluorescence (*C*). *A* displays the means ± S.E. of *n* = 3 independent experiments. *Arrows* depict nuclear rim staining indicative for nuclear pores. Mab414, anti–FG-repeat antibody. *Scale bar*, 10 μm. *NPC*, nuclear pore complex. *D*, PC3 cells transfected with increasing amounts of Nup214 siRNA were subjected to qPCR with primers specific for Nup214 and HES1. Displayed are the means of two independent experiments and S.E. *E*, PC3 cells transfected with 12× CSL luciferase Notch reporter were treated for 24 h with 10 μM DAPT and additionally 10 nM LMB where indicated and subjected to luciferase assay. Displayed are the means ± S.E. of *n* = 3 independent experiments. The *asterisk* indicates $p < 0.05$, Student's *t* test. *F* and *G*, C2C12 cells were transfected with 12× CSL luciferase Notch reporter and siRNAs as indicated. 24 h later, the cells were harvested and subjected to luciferase assay (*F*) or probed with indicated antibodies for protein expression (*G*). The graph displays the means ± S.E. from three independent experiments. The *asterisk* indicates $p < 0.05$, Students *t* test. For full-size blots of *B* and *G*, see supporting Fig. S6. *MW*, molecular mass.

Results and discussion

Knockdown of Nup88/214 increases Notch signaling in vitro and in vivo

Here we describe a novel role for the nuclear pore components Nup88 and Nup214 in Notch signaling. Using a constitutively active Notch (NotchΔE) tagged with EGFP (31), we screened siRNAs for modulators of Notch trafficking. Surprisingly, siRNAs against Nup214 did not change trafficking of NotchΔE/NICD-EGPF but increased Notch signaling.

To further get insights into the mechanism, we transfected human cells with siRNAs against Nup214 and a luciferase-based Notch reporter with 12× CSL-binding sites (31). Stability of Nup214 depends on its binding partner Nup88 (32), therefore knockdown (KD) of Nup88 was also tested. KD of either Nup strongly induced Notch signaling, whereas the KD of an unrelated Nup, Nup358, had only a small effect (Fig. 1A). The induction of Notch signaling upon KD of Nup88 or Nup214 was blocked by the γ-secretase inhibitor (GSI) DAPT (Fig. 1A). This suggests that the KD affects canonical NICD- and CSL/RBP-J–mediated Notch signaling.

All siRNAs specifically down-regulated their targets (Fig. 1B, additional siRNA against Nup214 was tested in Fig. S3, C and D). The KD of Nup88 influenced protein levels of Nup214 and vice versa, as published before (28, 33). Fig. 1C demonstrates that KD of Nup88 or Nup214 did not lead to general nuclear pore collapse, as indicated by staining with an anti–FG-repeat antibody (Mab414).

Because both KDs of Nup88 and Nup214 had the same effect, because of the mutual dependence, we focused on Nup214. We transfected increasing amounts of Nup214 siRNA and measured mRNA expression of Nup214 and a canonical Notch target, HES1 (34). Fig. 1D shows a dose-dependent KD of Nup214 mRNA and a concomitant HES1 up-regulation.

Nup214 plays a role in CRM1-mediated nuclear export (27, 28, 33), but a connection to Notch was not reported before. We therefore tested whether CRM1-mediated nuclear export is involved and inhibited this transport pathway by the selective CRM1 inhibitor leptomycin B (LMB) (35). Incubation of PC3 cells with LMB resulted in a similar, GSI-sensitive up-regulation of Notch signaling as the KD of Nup214 (Fig. 1E). The
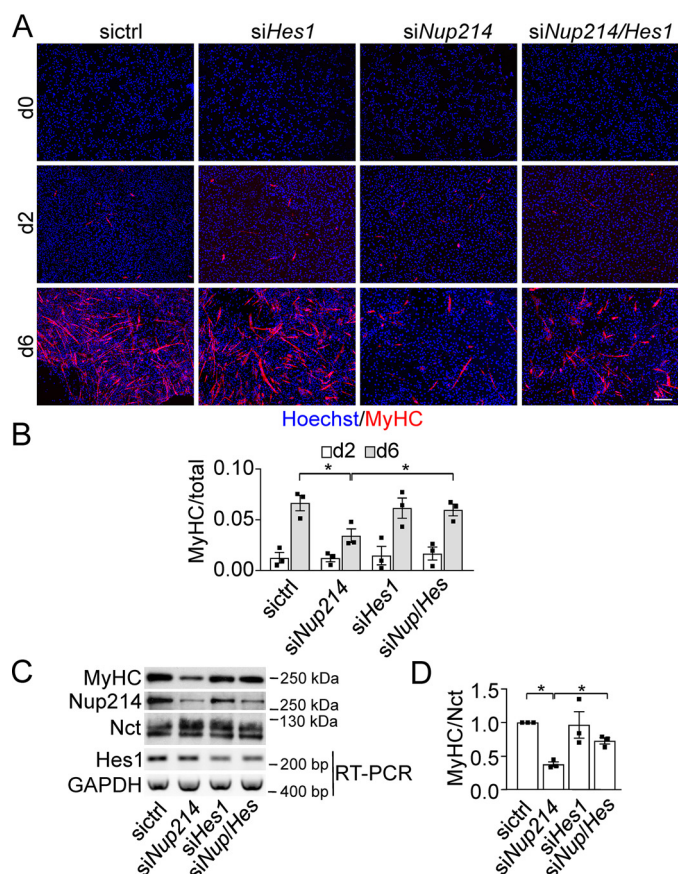
Figure 2. Nup214 KD delays or prevents differentiation of C2C12 cells. *A*, C2C12 cells transfected with siRNA as indicated were differentiated for 0, 2, and 6 days; fixed; and processed for immunofluorescence with MyHC antibodies. The nuclei were stained with Hoechst 33342. *Scale bar*, 200 μm. *B*, quantitation of at least 800 nuclei/condition. Displayed are the mean ratios $\pm$ S.E. from three independent experiments of MyHC positive to total cells. *C*, lysates from C2C12 cells treated as in *A* were immunoblotted for MyHC, Nup214, and Nicastrin (*Nct*), and mRNA levels were determined by RT-PCR for Hes1 and GAPDH. *D*, displays the relative intensities of MyHC to loading control Nct. siControl levels were set to 1. The graph displays means $\pm$ S.E. of three independent experiments. *Asterisks* indicate $p < 0.05$, Student's *t* test. For full-size blots of *C*, see supporting Fig. S6.

effects are not cell type–specific, because KD of Nup214 induced Notch signaling also in the mouse myoblast cell line C2C12 (Fig. 1, *F* and *G*). Together these results suggest that the CRM1–Nup214 axis is involved in regulating Notch signaling.

The CSL-luciferase assay in PC3 cells measured endogenous Notch signaling activity, but not its physiological consequences. We therefore analyzed the differentiation of C2C12 cells with or without KD of Nup214. Upon serum withdrawal, these cells differentiate into myotubes, and this differentiation is prevented by Notch signaling (36). KD of Nup214 inhibited proliferation of C2C12 cells (1.7-fold proliferation after 2 days in siControl-treated cells, −0.9-fold in siNup214 treated cells, $n = 3$ experiments), confirming earlier findings in HeLa cells (28). In addition KD of Nup214 delayed or reduced differentiation of C2C12 cells (Fig. 2*A*) as measured by the ratio of myosin heavy chain (MyHC) positive cells to total cells (Fig. 2*B*), the fusion index (not shown) and a reduction on MyHC protein levels (Fig. 2, *C* and *D*). Differentiation could be rescued by additional KD of Hes1, a major Notch downstream gene in myogenesis (37, 38), suggesting that the differentiation block by

KD of Nup214 was mediated via Notch signaling (Fig. 2, *A*–*D*). Taken together, the data suggested that KD of Nup214 prevented differentiation of C2C12 cells by increasing Notch signaling.

To analyze the role of Nup214 *in vivo*, we used zebrafish. In zebrafish, Notch signaling is involved in differentiation of many tissues, for example in notochord formation, somitogenesis, and hypochord specification (39). RT-PCR for the single zebrafish nup214 orthologue demonstrated that nup214 mRNA is maternally supplied to the zygote and that nup214 is strongly expressed in early stages of development (Fig. 3*A*). *In situ* hybridization confirmed the expression in early stages. After 17 h postfertilization and even more pronounced after 24 h postfertilization, nup214 displayed an increased tissue-specific expression pattern with strongest expression in the developing brain (Fig. 3*B*).

Interestingly, in adult zebrafish nup214 expression is restricted to a number of tissues like ovary, brain, kidney, and gills (Fig. 3, *C* and *D*). In the ovary, nup214 is expressed in oocytes of early stages, whereas in maturing oocytes nup214 message is localized in a stripe-like subcortical domain (Fig. 3*D*). Such asymmetrical localization was also observed for other maternally supplied mRNAs like notch (40). Of note, in *Arabidopsis*, the only other organism for which we found a tissue expressing study, the Nup214 orthologue LNO1 is also highly expressed in reproductive tissue and very low in vegetative tissue (41).

To address the function of nup214 in zebrafish development, we performed a morpholino (MO) based knockdown approach. RT-PCR analysis showed that injection of a MO targeting the splice donor site of exon 4 resulted in a dose-dependent reduction of correctly spliced nup214 mRNA (Fig. 3*E*).

To directly assess whether nup214 KD causes up-regulation of Notch activity in zebrafish, we analyzed the expression of *col2a1a* by *in situ* hybridization. Normally, *col2a1a* expressing cells are confined to a single cell layer in the trunk hypochord and floorplate of zebrafish embryos. After injection of the nup214 splice MO, *col2a1a* is expressed now also in the area of the trunk notochord (Fig. 3*F*, compare line scans of both conditions). As shown before (39), this expansion into the notochord area is a clear indication of Notch activation.

The knockdown effect was validated using a second nup214 MO that targets the 5′ UTR, interfering with translation (ATG MO; Fig. 3*E*). Injection of the ATG-MO dose-dependently induced the same expansion into the notochord as seen with the splice morpholino (Fig. S1). These data strongly suggested that Nup214 functions as a negative regulator of Notch signaling also *in vivo* during zebrafish development.

To further substantiate the *in vivo* data we analyzed an additional target of Notch, *her4* (42). Injection of the splice MO against Nup214 induced an up-regulation of *her4*, suggestive of an increased Notch signaling (Fig. S2).

Together, these data demonstrate that Nup88/214 negatively regulate Notch activity and, as LMB treatment has a similar effect, raise the intriguing possibility that Nup88/214 is involved in nuclear export of a Notch activator. KD of Nup88/214 (or LMB treatment) keeps this putative activator in the nucleus, resulting in increased Notch signaling.
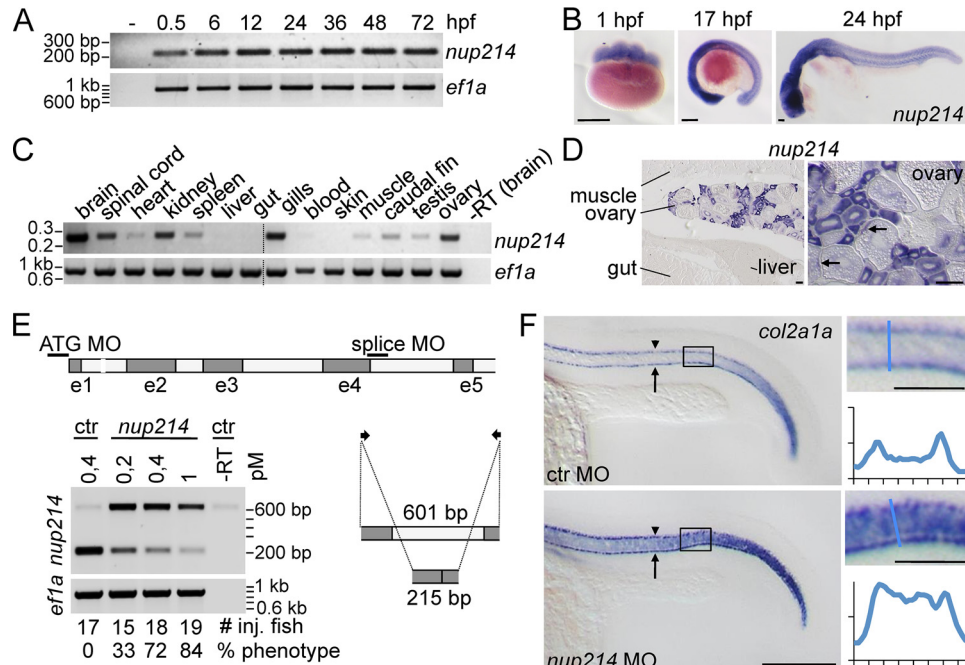
Figure 3. Nup214 is differentially expressed *in vivo* and negatively regulates Notch-signaling. *A–D*, expression analysis of Nup214 in zebrafish. *A*, RT-PCR with nup214-specific primers on zebrafish embryos and larvae from indicated time points. *B*, *in situ* hybridization of zebrafish embryos with a nup214-specific antisense probe. *Scale bar*, 150 μm. *C*, RT-PCR with nup214-specific primers on tissues from adult zebrafish tissues. *D*, *in situ* hybridization with a nup214 probe in adult zebrafish. *Arrows* point to localized mRNA in later stages of oogenesis. *Scale bar*, 100 μm. *E* and *F*, Nup214 inactivation by morpholinos activates Notch. *E*, scheme of nup214 pre-mRNA. *Black bars* indicate the binding site of the splice MO targeting exon 4/intron 4 splice site and the 5'-UTR MO (ATG MO). *Arrows* indicate the binding sites for the primers used to demonstrate the efficacy of knockdown, displayed in the agarose gel below. *215 bp*, correctly spliced mRNA; *601 bp*, mRNA with intron 4 inclusion. −*RT*, control condition without reverse transcriptase. Below the gel are the number of injected fish and the percentage of fish with the phenotype shown in *F*. *F*, whole mount *in situ* hybridization of *col2a1a* of 22-h-old zebrafish embryos injected with control or nup214 MOs (0.4 pM). For number of injected fish and percentage of phenotype, see *E*. The *boxed areas* are enlarged on the *right*, and the *line scans* at the indicated positions (*blue bars*) show intensity profiles (arbitrary units). *Arrowhead*, hypochord; *arrow*, floorplate. *Scale bar*, 200 μm, 50 μm in enlarged area. *ctr*, control.

Nup214 regulates Notch signaling via trafficking of RBP-J

An essential component of canonical Notch signaling is the DNA-binding factor RBP-J (CSL), which together with NICD forms the co-activator complex that drives Notch-dependent transcription (43). To test whether Nup214 is involved in RBP-J trafficking and whether this affects Notch-signaling, we used RBP-VP16, a RBP-J mutant that drives RBP-J/CSL-promoter genes independently of NICD (44). Transfection of RBP-VP16 in the presence or absence of GSI showed that it indeed induced transcription of a CSL-based luciferase reporter independent of NICD (Fig. 4*A*). KD of Nup214 further increased luciferase expression more than 3-fold, suggesting that Nup214 is directly or indirectly involved in nuclear trafficking of RBP-J.

To visualize this trafficking, C2C12 cells were treated with or without Nup214 siRNA and processed for immunofluorescence detection of endogenous RBP-J (see Fig. S3 for characterization of antibody). Quantification demonstrated that KD of Nup214 significantly shifted the distribution of RBP-J toward the nucleus (Fig. 4, *B* and *C*) while not changing total RBP-J levels (Fig. 4*D*).

More RBP-J in the nucleus does not necessarily mean more DNA binding, and not all RBP-J binding sites are dynamic (45, 46). We therefore performed ChIP-qPCR with an established RBP-J antibody (45) and analyzed known RBP-J binding sites in Notch target genes (45) compared with control regions (Fig. 4*E*). KD of Nup214 increased RBP-J binding to Notch target genes, but not to control regions. Very similar results were

obtained with a different RBP-J antibody (Fig. S4). Taken together, these data suggested that Nup214 negatively regulates Notch signaling by shuttling RBP-J out of the nucleus. KD of Nup214 increases the level of nuclear RBP-J and its binding to Notch target genes, thereby enhancing Notch activity.

LMB inhibits CRM1-dependent nuclear export, a major export route for proteins and RNA (47), and Nup214 is involved in CRM1-dependent nuclear export (28) of certain cargoes. To test whether KD of Nup214 would cause inhibition of all CRM1-dependent export, we determined the localization of activation-induced deaminase (AID)–GFP, a known CRM1 substrate (48), in PC3 cells. Although LMB clearly inhibited nuclear export of AID-GFP, KD of Nup88 or Nup214 did not, indicating that Nup88/214 are involved in the export of only a subset of CRM1-dependent proteins (Fig. 4, *F* and *G*).

Nup214 is up-regulated with increasing cell density (Fig. S5). This, together with the nonubiquitous, highly selective expression in zebrafish (Fig. 3, *B–D*) and *Arabidopsis* (41), suggests that Nup214 is not an essential core component of every nuclear pore but has specific roles in export of a subset of cargos. What remains to be shown is to what extent Nup214 isoforms are involved in context-specific transport.

Our data confirmed that Nup214 has a specific set of substrates (27, 28, 33). In agreement with this, expression levels of Nup214 were recently shown to be cell type–specific (49). Nup214 therefore belongs to the growing list of cell type/differentiation status–specific Nups (50–52).
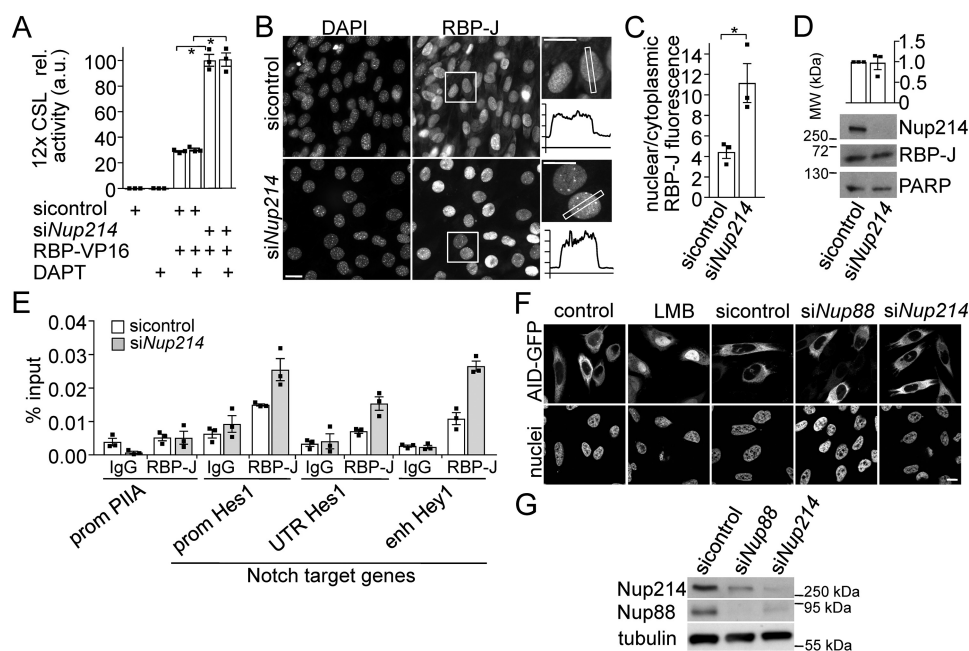
Figure 4. Nup214 exports RBP-J out of the nucleus. *A*, PC3 cells transfected with 12× CSL luciferase-based reporter and Notch-independent RBP-VP16 were transfected with control siRNA or Nup214 siRNA and treated with DAPT as indicated. Luciferase assays were performed after 72 h. The values from reporter and control-siRNA transfected cells were set to 1, and other conditions were related to that. Shown are the means ± S.E. of at least three independent experiments. *B*, localization of endogenous RBP-J with or without KD of endogenous Nup214 in C2C12 cells differentiated for 3 days was visualized by antibody staining and fluorescence microscopy. The *boxed areas* are magnified on the *right*, and examples of intensity profiles are shown. Note that the cytoplasmic intensity is halved in KD conditions. *C*, 180 cells from three independent experiments respectively were analyzed, and the ratio of extranuclear/nuclear RBP-J fluorescence was determined. Displayed are the means ± S.E. *D*, Western blotting of cells used in *B* and *C* probed with indicated antibodies. *Top row*, displayed is the mean RPB-J expression normalized to PARP and related to the siControl values set to 1. Displayed are the means ± S.E., $n = 3$ independent experiments. For full-size blots, see supporting Fig. S6. *E*, C2C12 cells transfected with control or Nup214 siRNA were subjected to ChIP-qPCR with RBP-J antibody (clone 1F1, Merck) and primers specific for a control region (*enh PIIA*) and three dynamic RBP-J binding sites (*prom Hes*, *UTR Hes*, and *enh Hey*). *Error bars* display the S.E. of three technical replicates. One of $n = 2$ independent experiments is shown. *F* and *G*, PC3 cells transfected with AID-GFP were transfected with control or Nup214 siRNA for 72 h or treated with 10 nM LMB for 24 h, fixed, and analyzed by immunofluorescence microscopy (*F*) or lysed and processed for immunoblotting with antibodies as indicated (*G*). For full-size blots, see supporting Fig. S6. *Asterisks* indicate $p < 0.05$, Student's *t* test. *Scale bars* in *B* and *F*, 10 μm. *MW*, molecular mass; *ctr*, control.

T-ALL associated Nup214 fusion proteins increase Notch signaling

In 50% of T-ALL the tumor is caused by aberrant Notch signaling (29). Interestingly, chromosomal translocations can cause or contribute to T-ALL in around 10% of cases. In all of these translocations, oncogenic fusions of proteins to Nup214 were detected (53–55). This raises the intriguing possibility that the Nup214-fusion proteins are loss-of-Nup214-function mutations that increase Notch signaling, contributing to malignancy.

To test this hypothesis, HEK293T cells were transfected with SET-Nup214, DEK-Nup214, and Nup214-ABL. SET and DEK are fused to the N terminus of Nup214, replacing parts of it. In Nup214-Abl, the Abl is fused to the C terminus of Nup214, replacing parts of it (53–55). After transfection of the fusion proteins, their effect on the distribution of endogenous Nup88 and 214 was assessed. HEK293 cells were used because of their suitability for nuclear pore immunostainings. Fig. 5*A* confirms that SET-Nup214 localized to nuclear, dense, brightly stained aggregates (56) that are in a dynamic equilibrium with the nucleoplasm (57). In contrast DEK-Nup214 localized to smaller, less bright, uniformly distributed aggregates, as shown before (56). Remarkably, SET-Nup214, but not DEK-Nup214 sequestered endogenous Nup88 and 214 to nuclear aggregates, diminishing their amounts at nuclear pores (Fig. 5*A*; quantification in Fig. 5*B*).

In contrast, Nup214-ABL, which contains the N terminus of Nup214, is recruited to nuclear pores and partially replaces endogenous Nup214 as published before (Fig. 6) (58). Nup88 is not changed under these conditions (Fig. 6). This "trapping" of endogenous Nup88/214 by SET-Nup214 away from the nuclear pores and the partial replacement of Nup214 by Nup214-ABL mimics the KD of Nup214 we described above. Therefore, we tested whether the expression of the fusion proteins would up-regulate Notch signaling. Indeed, in a CSL-dependent reporter assay, SET-Nup214 up-regulated Notch almost 4.6-fold, DEK-Nup214 up-regulated Notch 1.4-fold, and Nup214-ABL up-regulated Notch 2.9-fold (Fig. 5*C*). To analyze whether it is the Nup214 part that is responsible for the effect on Notch signaling, we replaced the fusion partners of Nup214 by GFP or an FK506-binding protein domain. In both cases the expression of the artificial fusion proteins resulted in a clear up-regulation of Notch, indicating that the Nup214-part of the fusion protein is causing the effect on Notch signaling (Fig. 5*C*).

Up-regulated Notch signaling is very important in T-ALL development (29). Our data suggest that in T-ALL patients with translocations resulting in Nup214 fusion proteins, an up-regulation of Notch could contribute to tumorigenesis. Our over-expression experiments with SET-Nup214 and DEK-Nup214 may exaggerate the patient situation.

Interestingly, the level of up-regulation of Notch coincides with the incidence of the respective mutations in T-ALL. SET-
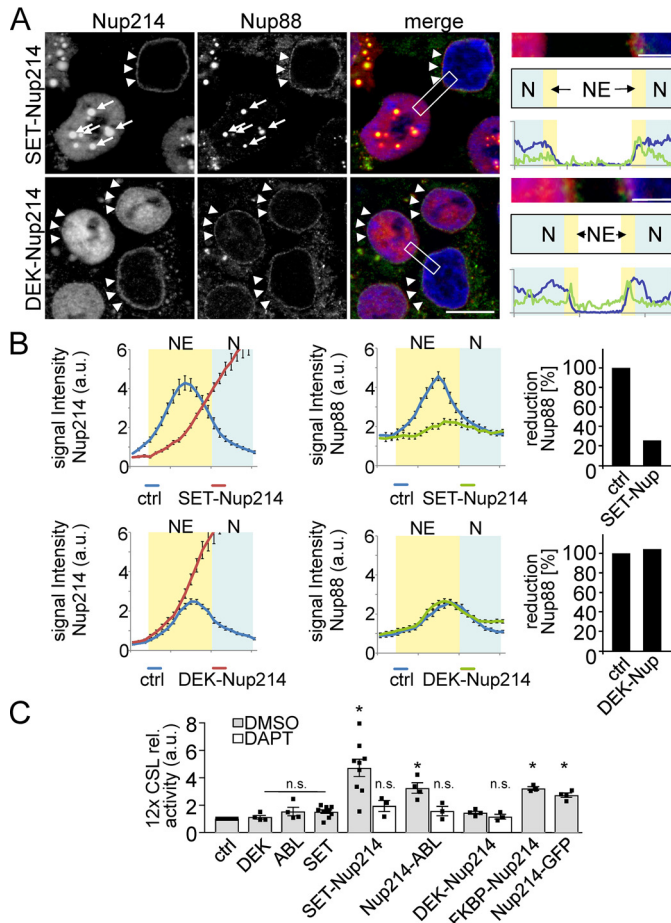
Figure 5. T-ALL causing Nup214 fusion proteins cause Notch up-regulation. *A*, PC3 cells transfected with SET-Nup214 or DEK-Nup214 were fixed after 24 h and processed for immunofluorescence with antibodies against Nup214 (staining the endogenous Nup214, as well as the overexpressed Nup214 fusion) and Nup88. *Arrows* depict SET-Nup214 nuclear aggregates; *arrowheads* indicate intact endogenous Nup88/214 staining at nuclear pores. Note that the SET-Nup214 aggregates in the Nup214 channel are overexposed to visualize also the endogenous Nup214 in the untransfected cell. The *boxed areas* in the merge images are enlarged on the *right panel* to demonstrate that SET-Nup214 but not DEK-Nup214 dislocates endogenous Nup88/214. The positions of nucleoplasm (*N*, *blue*) and nuclear envelope (*NE*, *yellow*) are schematized below, and line scans depicting Nup88 and DAPI staining are shown. *Scale bar* for *main panels*, 10 μm; *Scale bar* for *enlargements*, 2 μm. *B*, quantification using line scans of cells from *A*. 60 cells from *n* = 3 independent experiments were analyzed as described under "Experimental procedures." *Error bars* depict S.E. The percentage of Nup88 reduction refers to the area under the curves at the position of the NE, where control area was set to 100%. *C*, PC3 cells transfected with plasmids as indicated and 12× CSL luciferase reporter were processed for Notch activity detection. The activity in control (*ctrl*) cells was set to 1, and the other values were related to that. Displayed are the means ± S.E. of *n* = 3–9 independent experiments. *Asterisks* indicate significance (*p* < 0.05) related to control, Student's *t* test. *n.s.*, not significant.

Nup214, with the highest up-regulation of Notch, is found in 6% of T-ALL patients (59), followed by Nup214-ABL, in 5% (54), and finally DEK-Nup214, which only weakly influences Notch and is actually found in AML, not T-ALL (60). It should also be noted that Nup214 translocations are rarely found in patients with direct mutations of Notch (59).

In summary, we showed that the nuclear pore components Nup88/214 negatively regulate Notch signaling *in vitro* and *in vivo* in zebrafish. Although the importance of the nuclear transport machinery and its regulation/misregulation in develop-
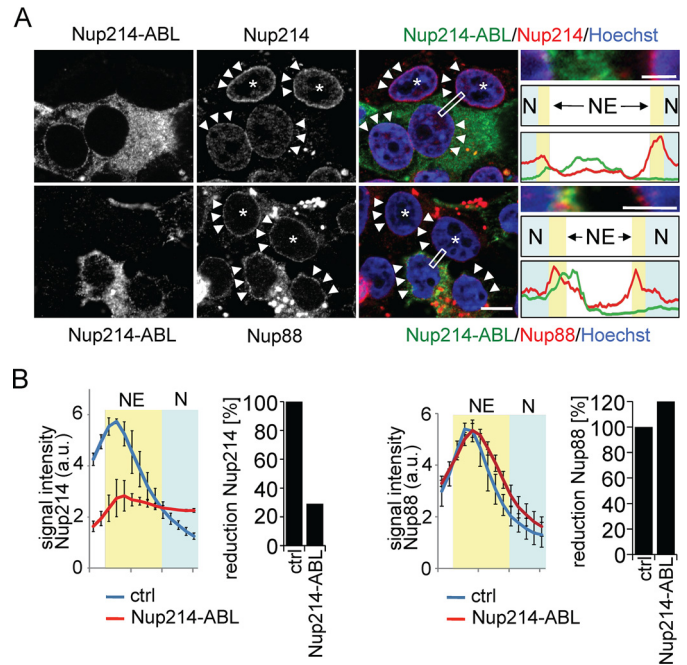

Figure 6. Nup214-ABL displaces endogenous Nup214 but not Nup88. *A*, HEK293T cells were transfected with Nup214-ABL, fixed after 24 h, and processed for immunofluorescence against myc (the epitope in Nup214 recognized by the Nup214 antibody we use is deleted) and Nup88 or Nup214 as indicated. Nuclear pore localization was determined as depicted in Fig. 5. Note that transfected cells show clear loss of fluorescence signal of Nup214 at the nuclear rim (*arrowheads*, *upper panel*) but not of Nup88 (*arrowheads*, *lower panel*). *Asterisk*, untransfected cells. *Scale bar* for *main panels*, 10 μm; *Scale bar* for *enlargements*, 2 μm. The *boxed areas* in the merge images are enlarged in the *right panel*. The positions of nucleoplasm (*N*, *blue*) and nuclear envelope (*NE*, *yellow*) are schematized, and line scans depicting Nup214-ABL (*green*), Nup214 (*red*, *upper graph*), or Nup88 (*red*, *lower graph*) are shown. *B*, quantification using line scans of cells from *A*. 60–80 cells from *n* = 3 independent experiments were analyzed as described under "Experimental procedures." *Error bars* depict S.E. The percentage of Nup88/214 reduction refers to the area under the curves at the position of the NE (*yellow*), where the control area was set to 100%. *ctrl* refers to untransfected cells.

ment and disease has been widely appreciated (reviewed in Refs. 52, 61, and 62), its importance in Notch signaling was not yet recognized. Our data suggest that nuclear RBP-J is rate-limiting for Notch signaling and that regulation of nucleocytoplasmic transport is an additional measure for fine-tuning Notch activity, adding another level of complexity to an already complex signaling mechanism.

Inhibiting nuclear export is a promising strategy in cancer therapy (63, 64). However, an unwanted side effect might be an up-regulation of Notch signaling, which, given its role in proliferation and cancer, could be detrimental. It remains to be shown to what extent the up-regulation of Notch by oncogenic Nup214 fusion proteins indeed contributes to tumorigenesis of T-ALL and/or whether additional functions of Nup88/214 like mRNA export (27, 28, 57, 65) are involved.

Experimental procedures

For antibodies, primers, and morpholino sequences, see Tables S1 and S2.

Cell lines

HeLa Kyoto, HEK293T, C2C12 (ATCC CRL-1772), PC3 (ATCC® CRL-1435™), cells were maintained in Dulbecco's modified Eagle's medium + GlutaMAX (Invitrogen) supple-

mented with 10% FBS and incubated at 37 °C, 95% relative humidity, and 5% CO_2.

Quantitative RT-PCR

Expression levels of Nup214 and HES1 mRNA were quantified using real-time PCR according to standard protocols. cDNAs were reverse-transcribed from 2 μg of total RNA. The PCR (denaturation 95 °C for 2 min followed by 40 cycles of 95 °C for 15 s and 60 °C for 1 min) was performed using Sybr Green PCR Core Reagents (PE Applied Biosystems).

Nup214 fusion plasmids

DEK-Nup214 (66) was kindly provided by Carl Sandén from LUND University and was subcloned in via EagI restriction site into pCMV-Myc. Human DEK cDNA (accession no. 5122743, Invitrogen) was subcloned via EcoRI and XhoI restriction sites into pCMV-Myc. SET-Nup214 according to the sequence published in Ref. 53 was constructed by overlap extension PCR and cloned in pcDNA4/myc-HisA vector (Invitrogen). The SET coding sequence up to the end of exon7 was amplified using Phusion polymerase (Fynnzymes) and primers SET-F and SET-Nup-R from a MGC verified human SET cDNA clone (accession no. 5587291, Thermo Scientific). The Nup214 coding sequence starting from exon 18 was amplified from a human Nup214 full-length construct using primers SET-Nup-F and Nup214-R. Nup214-ABL, Nup214-GFP, and FKBP-Nup214 were constructed via Gibson assembly cloning kit (NEB), and primers were generated with NEBuilder®. For Nup214-ABL (sequence according to Ref. 54), Nup214 was amplified from start codon to exon29 and ABL1 from exon2 to stop codon from an ABL1 cDNA in pCR TOPO2.1 isolated from PC3 lysates. The sequences were assembled together with pcDNA3.1-Myc vector (Invitrogen). For Nup214-GFP the same Nup214 sequence was amplified as for Nup214-ABL. GFP was amplified from pEGFP-C1 vector, and the fragments were assembled together with EcoRI and XhoI digested pcDNA3.1 vector. For FKBP-Nup214 the same Nup214 sequence was amplified as for SET-Nup214 or DEK-Nup214, FKBP was amplified from pC4-Fv2E vector (Clontech), and the fragments were assembled together with StuI- and XhoI-digested pCMV-Myc vector. All vectors contain a cytomegalovirus promotor. All primer sequences are listed in the supporting information.

Reporter assays

Notch activity was analyzed using a 12× CSL-luciferase plasmid as described before (31). Briefly, for KD experiments PC3 cells plated in a 24-well format were transfected for 2 days with 10 nM siRNA (siCtrl), siNUP214, siNUP88 (SMARTpool, Thermo Fisher), siNUP358 (ON-TARGET plus, Dharmacon) using Dharmafect followed by plasmid transfection using Lipofectamine 2000 (Invitrogen), 300 ng of pGL4.20−12× CSL-luciferase reporter plasmid, and 6 ng of pGL4.74-[hRluc/TK] *Renilla* luciferase internal control plasmid. Firefly and *Renilla* luciferase activities were measured in cell lysates prepared 24 h after transfection with the Promega Dual-Luciferase kit via manufacturer's instructions, using a Mithras LB 940.

For NUP214 fusion overexpression experiments, PC3 cells were plated in 6-well format and transfected for 24 h with

equimolar Plasmid DNA and 500 ng of pGL4.20−12× CSL-luciferase reporter plasmid using Polyethylenglycol (PEI). Firefly luciferase activity was measured in cell lysates prepared 24 h after transfection with the Promega Dual-Luciferase kit. Firefly values were normalized against the protein content analyzed with Pierce BCA protein assay kit via the manufacturer's instructions, using a Mithras LB 940.

C2C12 transfection and differentiation

Control siRNA or Nup214 or Hes1 siRNA (details in the supporting information) were transfected in C2C12 cells by using Amaxa® Cell Line Nucleofector® kit V and the Nucleofector® II device (Lonza). For differentiation, the cells were plated at a density of 6 × 104 cells/cm^2 and starved in DMEM with 1% FCS. For quantification of differentiation, MyHC-positive cells were counted manually with ImageJ and Hoechst-stained nuclei automatically with CellProfiler. The ratios of MyHC-positive/total number of cells, subtracted with the value for d.0 of differentiation, were calculated.

Immunocytochemistry and microscopy of cells

For immunofluorescence cells were grown on coverslips. After incubation the cells were fixed with 4% formalin and processed for immunofluorescence with antibodies as indicated. The nuclei were stained with Hoechst 33342 (Invitrogen H1399). Images were acquired on a Zeiss Axiovert200 using 40× or 63× objective and Axiovision and Zen2012 software. For some settings a confocal-like Apotome slider was used. For the quantification of the nuclear-cytoplasmic ratio of RBP-J, images were analyzed in ZEN2012 software (Zeiss). The bar scan tool was applied across single cells (30 cells per condition per experiment), and the resulting signal intensity profiles were exported to Excel 2010 (Microsoft). The RBP-J signal intensity in the cytoplasm and in the nucleus was averaged, and the ratio was calculated. To avoid ambiguities in allocation of intensities to either nucleus or cytoplasm at the transition nucleus–cytoplasm, RBP-J signals from that area were excluded from the calculations. The transition region was defined to be 0.25 μm in both directions of the line where the Hoechst signal is half-maximal. Images were assembled and processed in Adobe Photoshop. In some cases nonlinear γ-settings of <1 were used to match the image perception by eye, but care was taken that identical settings were applied to conditions from the same experiment.

Zebrafish maintenance and staging

WT zebrafish (strain AB Tübingen) were maintained under standard conditions for zebrafish husbandry (67). Embryos were staged according to morphological criteria (68).

Morpholino antisense oligonucleotides

Nup214 MOs (Gene Tools, LLC, Philomath, OR) were designed to target either the translational start (nup214 ATG) or the splice donor site of exon 4 (nup214 splice). As a negative control a standard MO that targets a human β-globin intron mutation was used. MOs were diluted in water to a working concentration of 1 mM with 0.05% phenol red (Sigma) as a tracer. Injections into the yolk of 1- or 2-cell embryos were

performed using a manual micromanipulator (type M1, Saur, Germany). For each MO different volumes were injected, calculated by using a graticule (Pyser-SGI, Edenbridge, UK). To analyze knockdown efficiency of the splice MO, total RNA was isolated from 24-h-old zebrafish embryos using the RNeasy mini kit (Qiagen), reverse-transcribed with the iScriptTM cDNA synthesis kit (Bio-Rad), and analyzed by RT-PCR.

In situ hybridization

For generation of the nup214 probe, a cDNA fragment comprising exons 1–6 served as a template. The col2a1a probe (69) was generously provided by John H. Postlethwait (University of Oregon). The cDNA fragment that was used to synthesize the antisense RNA probe for *her4.1* was amplified with the following primers: AGAAAGCCCATGGTGGAGAAG (forward), GCTTTCCATTGTTGCTTGATTGTA (reverse) and gave rise to an 785-bp amplicon. Whole-mount *in situ* hybridizations were carried out as previously described (70). *In 1situ* hybridization on longitudinal sections of adult zebrafish was performed essentially as described (71). Images were captured using a SteREO Discovery.V8 microscope (Zeiss) equipped with an Achromat-S objectives and an AxioCam MRC camera using the AxioVision software. Images were processed with Adobe Photoshop. Intensity profiles were obtained using Zen software (Zeiss).

ChIP-qPCR

ChIP was performed on 3 days serum-starved (DMEM + 1% FBS) C2C12 cells. The cells from three 10-cm dishes were fixed with 1% formaldehyde in $1\times$ PBS at room temperature for 10 min, quenched with 0.125 M glycin for 5 min, washed two times with ice-cold $1\times$ PBS, and harvested in ice-cold PBS containing Protease inhibitor mixture. To release the nuclei, the cells were pelleted at 500 relative centrifugal force for 10 min at 4 °C and resuspended in 5 ml of hypotonic buffer (20 mM Tris, pH 7.4, 2 mM $MgCl_2$, 5% glycerol) containing protease inhibitor cocktail and 0.6% Nonidet P-40. The suspension was incubated on ice for 4 min with occasional mild vortexing. The nuclei were pelleted at 1000 rcf for 5 min at 4 °C and resuspended in ChIP lysis buffer (50 mM HEPES-KOH, pH 7.5, 140 mM NaCl, 1 mM EDTA, pH 8, 1% Triton X-100, 0.1% sodium deoxycholate, 0.1% SDS) for 10 min. The lysate was sonicated to shear the DNA into 300–800-bp fragments. The protein–DNA complexes were detected using 30–35 μg of DNA and 5 μg of Ab against RBP-J (clone 1F1; Merck Chemicals; MABE982 or Abcam; ab25949) or isotype control (rat IgG) in 1 ml of chip lysis buffer and incubated for 1 h at 4 °C under rotating conditions. The complexes were precipitated by an overnight incubation at 4 °C on a rotator with 30 μl of magnetic Dynabeads protein G (Thermo Fischer). The protein–DNA complexes were washed two times for 5 min with low-salt wash buffer (0.1% SDS, 1% Triton X-100, 2 mM EDTA, 20 mM Tris-HCl, pH 8.0, 150 mM NaCl) followed by high salt (0.1% SDS, 1% Triton X-100, 2 mM EDTA, 20 mM Tris-HCl, pH 8.0, 500 mM NaCl) and LiCl (0.25 M LiCl, 1% Nonidet P-40, 1% sodium deoxycholate, 1 mM EDTA, 10 mM Tris-HCl, pH 8.0) wash buffer always by incubating at 4 °C on a rotation wheel. The protein–DNA complexes were eluted and reverse cross-linked, and the DNA was purified via phenol chloroform extraction. The specific DNA enrichment was quantified by real-time PCR.

Statistics

Arithmetic means of the numerical data were compared using the Student's *t* test. A difference in means was considered statistically significant as indicated in the figures. *Error bars* depict the S.E., and numbers of independent replicates are indicated in the figure legends.

References

1. Artavanis-Tsakonas, S., Matsuno, K., and Fortini, M. (1995) Notch signaling. *Science* **268**, 225–232 CrossRef Medline
2. Bray, S. J. (2006) Notch signalling: a simple pathway becomes complex. *Nat. Rev. Mol. Cell Biol.* **7**, 678–689 CrossRef Medline
3. Fiúza, U.-M., and Arias, A. M. (2007) Cell and molecular biology of Notch. *J. Endocrinol.* **194**, 459–474 CrossRef Medline
4. Logeat, F., Bessia, C., Brou, C., LeBail, O., Jarriault, S., Seidah, N. G., and Israël, A. (1998) The Notch1 receptor is cleaved constitutively by a furin-like convertase. *Proc. Natl. Acad. Sci.* **95**, 8108–8112 CrossRef Medline
5. Brou, C., Logeat, F., Gupta, N., Bessia, C., LeBail, O., Doedens, J. R., Cumano, A., Roux, P., Black, R. A., and Israël, A. (2000) A novel proteolytic cleavage involved in Notch signaling: the role of the disintegrin-metalloprotease TACE. *Mol. Cell* **5**, 207–216 CrossRef Medline
6. De Strooper, B., Annaert, W., Cupers, P., Saftig, P., Craessaerts, K., Mumm, J. S., Schroeter, E. H., Schrijvers, V., Wolfe, M. S., Ray, W. J., Goate, A., and Kopan, R. (1999) A presenilin-1-dependent γ-secretase-like protease mediates release of Notch intracellular domain. *Nature* **398**, 518–522 CrossRef Medline
7. Borggrefe, T., and Oswald, F. (2009) The Notch signaling pathway: transcriptional regulation at Notch target genes. *Cell. Mol. Life Sci.* **66**, 1631–1646 CrossRef Medline
8. Kopan, R., and Ilagan, M. X. (2009) The canonical Notch signaling pathway: unfolding the activation mechanism. *Cell* **137**, 216–233 CrossRef Medline
9. Kim, M.-Y., Ann, E.-J., Kim, J.-Y., Mo, J.-S., Park, J.-H., Kim, S.-Y., Seo, M.-S., and Park, H.-S. (2007) Tip60 histone acetyltransferase acts as a negative regulator of Notch1 signaling by means of acetylation. *Mol. Cell Biol.* **27**, 6506–6519 CrossRef Medline
10. Acar, M., Jafar-Nejad, H., Takeuchi, H., Rajan, A., Ibrani, D., Rana, N. A., Pan, H., Haltiwanger, R. S., and Bellen, H. J. (2008) Rumi is a CAP10 domain glycosyltransferase that modifies Notch and is required for Notch signaling. *Cell* **132**, 247–258 CrossRef Medline
11. Hein, K., Mittler, G., Cizelsky, W., Kühl, M., Ferrante, F., Liefke, R., Berger, I. M., Just, S., Sträng, J. E., Kestler, H. A., Oswald, F., and Borggrefe, T. (2015) Site-specific methylation of Notch1 controls the amplitude and duration of the Notch1 response. *Sci. Signal.* **8**, ra30 CrossRef Medline

12. Le Bras, S., Loyer, N., and Le Borgne, R. (2011) The multiple facets of ubiquitination in the regulation of Notch signaling pathway. *Traffic* **12,** 149–161 CrossRef Medline

13. Wu, G., Lyapina, S., Das, I., Li, J., Gurney, M., Pauley, A., Chui, I., Deshaies, R. J., and Kitajewski, J. (2001) SEL-10 is an inhibitor of Notch signaling that targets Notch for ubiquitin-mediated protein degradation. *Mol. Cell Biol.* **21,** 7403–7415 CrossRef Medline

14. Oberg, C., Li, J., Pauley, A., Wolf, E., Gurney, M., and Lendahl, U. (2001) The Notch intracellular domain is ubiquitinated and negatively regulated by the mammalian Sel-10 homolog. *J. Biol. Chem.* **276,** 35847–35853 CrossRef Medline

15. Gupta-Rossi, N., Le Bail, O., Gonen, H., Brou, C., Logeat, F., Six, E., Ciechanover, A., and Israël, A. (2001) Functional interaction between SEL-10, an F-box protein, and the nuclear form of activated Notch1 receptor. *J. Biol. Chem.* **276,** 34371–34378 CrossRef Medline

16. McGill, M. A., and McGlade, C. J. (2003) Mammalian numb proteins promote Notch1 receptor ubiquitination and degradation of the Notch1 intracellular domain. *J. Biol. Chem.* **278,** 23196–23203 CrossRef Medline

17. Ishitani, T., Hirao, T., Suzuki, M., Isoda, M., Ishitani, S., Harigaya, K., Kitagawa, M., Matsumoto, K., and Itoh, M. (2010) Nemo-like kinase suppresses Notch signalling by interfering with formation of the Notch active transcriptional complex. *Nat. Cell Biol.* **12,** 278–285 CrossRef Medline

18. Fryer, C. J., White, J. B., and Jones, K. A. (2004) Mastermind recruits CycC:CDK8 to phosphorylate the Notch ICD and coordinate activation with turnover. *Mol. Cell* **16,** 509–520 CrossRef Medline

19. Song, J., Park, S., Kim, M., and Shin, I. (2008) Down-regulation of Notch-dependent transcription by Akt in vitro. *FEBS Lett.* **582,** 1693–1699 CrossRef Medline

20. Ranganathan, P., Vasquez-Del Carpio, R., Kaplan, F. M., Wang, H., Gupta, A., VanWye, J. D., and Capobianco, A. J. (2011) Hierarchical phosphorylation within the ankyrin repeat domain defines a phosphoregulatory loop that regulates Notch transcriptional activity. *J. Biol. Chem.* **286,** 28844–28857 CrossRef Medline

21. Fassa, A., Parisiadou, L., Robakis, N. K., and Efthimiopoulos, S. (2007) Novel processing of Notch 1 within its intracellular domain by a cysteine protease. *Neurodegener. Dis.* **4,** 148–155 CrossRef Medline

22. Tagami, S., Okochi, M., Yanagida, K., Ikuta, A., Fukumori, A., Matsumoto, N., Ishizuka-Katsura, Y., Nakayama, T., Itoh, N., Jiang, J., Nishitomi, K., Kamino, K., Morihara, T., Hashimoto, R., Tanaka, T., *et al.* (2008) Regulation of Notch signaling by dynamic changes in the precision of S3 cleavage of Notch-1. *Mol. Cell Biol.* **28,** 165–176 CrossRef Medline

23. Pumroy, R. A., and Cingolani, G. (2015) Diversification of importin-α isoforms in cellular trafficking and disease states. *Biochem. J.* **466,** 13–28 CrossRef Medline

24. Cautain, B., Hill, R., de Pedro, N., and Link, W. (2015) Components and regulation of nuclear transport processes. *FEBS J.* **282,** 445–462 CrossRef Medline

25. van Deursen, J., Boer, J., Kasper, L., and Grosveld, G. (1996) G2 arrest and impaired nucleocytoplasmic transport in mouse embryos lacking the proto-oncogene CAN/Nup214. *EMBO J.* **15,** 5574–5583 CrossRef Medline

26. Trotman, L. C., Mosberger, N., Fornerod, M., Stidwill, R. P., and Greber, U. F. (2001) Import of adenovirus DNA involves the nuclear pore complex receptor CAN/Nup214 and histone H1. *Nat. Cell Biol.* **3,** 1092–1100 CrossRef Medline

27. Bernad, R., Engelsma, D., Sanderson, H., Pickersgill, H., and Fornerod, M. (2006) Nup214-Nup88 nucleoporin subcomplex is required for CRM1-mediated 60 S preribosomal nuclear export. *J. Biol. Chem.* **281,** 19378–19386 CrossRef Medline

28. Hutten, S., and Kehlenbach, R. H. (2006) Nup214 is required for CRM1-dependent nuclear protein export *in vivo*. *Mol. Cell. Biol.* **26,** 6772–6785 CrossRef Medline

29. Koch, U., and Radtke, F. (2011) Notch in T-ALL: new players in a complex disease. *Trends Immunol.* **32,** 434–442 CrossRef Medline

30. Belver, L., and Ferrando, A. (2016) The genetics and mechanisms of T cell acute lymphoblastic leukaemia. *Nat. Rev. Cancer* **16,** 494–507 CrossRef Medline

31. Huenniger, K., Krämer, A., Soom, M., Chang, I., Köhler, M., Depping, R., Kehlenbach, R. H., and Kaether, C. (2010) Notch1 signaling is mediated by importins α 3, 4, and 7. *Cell Mol. Life Sci.* **67,** 3187–3196 CrossRef Medline

32. Fornerod, M., van Deursen, J., van Baal, S., Reynolds, A., Davis, D., Murti, K. G., Fransen, J., and Grosveld, G. (1997) The human homologue of yeast CRM1 is in a dynamic subcomplex with CAN/Nup214 and a novel nuclear pore component Nup88. *EMBO J.* **16,** 807–816 CrossRef Medline

33. Bernad, R., van der Velde, H., Fornerod, M., and Pickersgill, H. (2004) Nup358/RanBP2 attaches to the nuclear pore complex via association with Nup88 and Nup214/CAN and plays a supporting role in CRM1-mediated nuclear protein export. *Mol. Cell. Biol.* **24,** 2373–2384 CrossRef Medline

34. Sasai, Y., Kageyama, R., Tagawa, Y., Shigemoto, R., and Nakanishi, S. (1992) Two mammalian helix–loop–helix factors structurally related to *Drosophila* hairy and enhancer of split. *Genes Dev.* **6,** 2620–2634 CrossRef Medline

35. Kudo, N., Wolff, B., Sekimoto, T., Schreiner, E. P., Yoneda, Y., Yanagida, M., Horinouchi, S., and Yoshida, M. (1998) Leptomycin B inhibition of signal-mediated nuclear export by direct binding to CRM1. *Exp. Cell Res.* **242,** 540–547 CrossRef Medline

36. Kopan, R., Nye, J. S., and Weintraub, H. (1994) The intracellular domain of mouse Notch: a constitutively activated repressor of myogenesis directed at the basic helix–loop–helix region of MyoD. *Development* **120,** 2385–2396 Medline

37. Kuroda, K., Tani, S., Tamura, K., Minoguchi, S., Kurooka, H., and Honjo, T. (1999) Delta-induced Notch signaling mediated by RBP-J inhibits MyoD expression and myogenesis. *J. Biol. Chem.* **274,** 7238–7244 CrossRef Medline

38. Lahmann, I., Bröhl, D., Zyrianova, T., Isomura, A., Czajkowski, M. T., Kapoor, V., Griger, J., Ruffault, P. L., Mademtzoglou, D., Zammit, P. S., Wunderlich, T., Spuler, S., Kühn, R., Preibisch, S., Wolf, J., *et al.* (2019) Oscillations of MyoD and Hes1 proteins regulate the maintenance of activated muscle stem cells. *Genes Dev.* **33,** 524–535 CrossRef Medline

39. Latimer, A. J., and Appel, B. (2006) Notch signaling regulates midline cell specification and proliferation in zebrafish. *Dev. Biol.* **298,** 392–402 CrossRef Medline

40. Bally-Cuif, L., Schatz, W. J., and Ho, R. K. (1998) Characterization of the zebrafish Orb/CPEB-related RNA binding protein and localization of maternal components in the zebrafish oocyte. *Mech. Dev.* **77,** 31–47 CrossRef Medline

41. Braud, C., Zheng, W., and Xiao, W. (2012) LONO1 encoding a nucleoporin is required for embryogenesis and seed viability in *Arabidopsis*. *Plant Physiol.* **160,** 823–836 CrossRef Medline

42. Takke, C., Dornseifer, P., v Weizsäcker, E., and Campos-Ortega, J. A. (1999) her4, a zebrafish homologue of the *Drosophila* neurogenic gene E(spl), is a target of NOTCH signalling. *Development* **126,** 1811–1821 Medline

43. Tamura, K., Taniguchi, Y., Minoguchi, S., Sakai, T., Tun, T., Furukawa, T., and Honjo, T. (1995) Physical interaction between a novel domain of the receptor Notch and the transcription factor RBP-Jκ/Su(H). *Curr. Biol.* **5,** 1416–1423 CrossRef Medline

44. Waltzer, L., Bourillot, P. Y., Sergeant, A., and Manet, E. (1995) RBP-Jκ repression activity is mediated by a co-repressor and antagonized by the Epstein–Barr virus transcription factor EBNA2. *Nucleic Acids Res.* **23,** 4939–4945 CrossRef Medline

45. Castel, D., Mourikis, P., Bartels, S. J., Brinkman, A. B., Tajbakhsh, S., and Stunnenberg, H. G. (2013) Dynamic binding of RBPJ is determined by Notch signaling status. *Genes Dev.* **27,** 1059–1071 CrossRef Medline

46. Wang, H., Zang, C., Taing, L., Arnett, K. L., Wong, Y. J., Pear, W. S., Blacklow, S. C., Liu, X. S., and Aster, J. C. (2014) NOTCH1-RBPJ complexes drive target gene expression through dynamic interactions with superenhancers. *Proc. Natl. Acad. Sci. U.S.A.* **111,** 705–710 CrossRef Medline

47. Hutten, S., and Kehlenbach, R. H. (2007) CRM1-mediated nuclear export: to the pore and beyond. *Trends Cell Biol* **17,** 193–201 CrossRef Medline

48. McBride, K. M., Barreto, V., Ramiro, A. R., Stavropoulos, P., and Nussenzweig, M. C. (2004) Somatic hypermutation is limited by CRM1-depen-

dent nuclear export of activation-induced deaminase. *J. Exp. Med.* **199,** 1235–1244 CrossRef Medline

49. Ori, A., Banterle, N., Iskar, M., Andrés-Pons, A., Escher, C., Khanh Bui, H., Sparks, L., Solis-Mezarino, V., Rinner, O., Bork, P., Lemke, E. A., and Beck, M. (2013) Cell type-specific nuclear pores: a case in point for context-dependent stoichiometry of molecular machines. *Mol. Syst. Biol.* **9,** 648 Medline

50. D'Angelo, M. A., Gomez-Cavazos, J. S., Mei, A., Lackner, D. H., and Hetzer, M. W. (2012) A change in nuclear pore complex composition regulates cell differentiation. *Dev. Cell* **22,** 446–458 CrossRef Medline

51. Raices, M., and D'Angelo, M. A. (2012) Nuclear pore complex composition: a new regulator of tissue-specific and developmental functions. *Nat. Rev. Mol. Cell Biol.* **13,** 687–699 CrossRef Medline

52. Gomez-Cavazos, J. S., and Hetzer, M. W. (2012) Outfits for different occasions: tissue-specific roles of nuclear envelope proteins. *Curr. Opin. Cell Biol.* **24,** 775–783 CrossRef Medline

53. Van Vlierberghe, P., van Grotel, M., Tchinda, J., Lee, C., Beverloo, H. B., van der Spek, P. J., Stubbs, A., Cools, J., Nagata, K., Fornerod, M., Buijs-Gladdines, J., Horstmann, M., van Wering, E. R., Soulier, J., Pieters, R., *et al.* (2008) The recurrent SET-NUP214 fusion as a new HOXA activation mechanism in pediatric T-cell acute lymphoblastic leukemia. *Blood* **111,** 4668–4680 CrossRef Medline

54. Graux, C., Cools, J., Melotte, C., Quentmeier, H., Ferrando, A., Levine, R., Vermeesch, J. R., Stul, M., Dutta, B., Boeckx, N., Bosly, A., Heimann, P., Uyttebroeck, A., Mentens, N., Somers, R., *et al.* (2004) Fusion of NUP214 to ABL1 on amplified episomes in T-cell acute lymphoblastic leukemia. *Nat. Genet.* **36,** 1084–1089 CrossRef Medline

55. Gorello, P., La Starza, R., Di Giacomo, D., Messina, M., Puzzolo, M. C., Crescenzi, B., Santoro, A., Chiaretti, S., and Mecucci, C. (2010) SQSTM1-NUP214: a new gene fusion in adult T-cell acute lymphoblastic leukemia. *Haematologica* **95,** 2161–2163 CrossRef Medline

56. Fornerod, M., Boer, J., van Baal, S., Jaeglé, M., von Lindern, M., Murti, K. G., Davis, D., Bonten, J., Buijs, A., and Grosveld, G. (1995) Relocation of the carboxyterminal part of CAN from the nuclear envelope to the nucleus as a result of leukemia-specific chromosome rearrangements. *Oncogene* **10,** 1739–1748 Medline

57. Port, S. A., Mendes, A., Valkova, C., Spillner, C., Fahrenkrog, B., Kaether, C., and Kehlenbach, R. H. (2016) The oncogenic fusion proteins SET-Nup214 and sequestosome-1 (SQSTM1)-Nup214 form dynamic nuclear bodies and differentially affect nuclear protein and poly(A)$^+$ RNA export. *J. Biol. Chem.* **291,** 23068–23083 CrossRef Medline

58. De Keersmaecker, K., Rocnik, J. L., Bernad, R., Lee, B. H., Leeman, D., Gielen, O., Verachtert, H., Folens, C., Munck, S., Marynen, P., Fornerod, M., Gilliland, D. G., and Cools, J. (2008) Kinase activation and transformation by NUP214-ABL1 is dependent on the context of the nuclear pore. *Mol. Cell* **31,** 134–142 CrossRef Medline

59. Ben Abdelali, R., Roggy, A., Leguay, T., Cieslak, A., Renneville, A., Touzart, A., Banos, A., Randriamalala, E., Caillot, D., Lioure, B., Devidas, A., Mossafa, H., Preudhomme, C., Ifrah, N., Dombret, H., *et al.* (2014) SET-NUP214 is a recurrent gammadelta lineage-specific fusion transcript associated with corticosteroid/chemotherapy resistance in adult T-ALL. *Blood* **123,** 1860–1863 CrossRef Medline

60. von Lindern, M., Fornerod, M., van Baal, S., Jaegle, M., de Wit, T., Buijs, A., and Grosveld, G. (1992) The translocation (6;9), associated with a specific subtype of acute myeloid leukemia, results in the fusion of two genes, dek and can, and the expression of a chimeric, leukemia-specific dek-can mRNA. *Mol. Cell. Biol.* **12,** 1687–1697 CrossRef Medline

61. Poon, I. K., and Jans, D. A. (2005) Regulation of nuclear transport: central role in development and transformation? *Traffic* **6,** 173–186 CrossRef Medline

62. Köhler, A., and Hurt, E. (2010) Gene regulation by nucleoporins and links to cancer. *Mol. Cell* **38,** 6–15 CrossRef Medline

63. Gravina, G. L., Senapedis, W., McCauley, D., Baloglu, E., Shacham, S., and Festuccia, C. (2014) Nucleo-cytoplasmic transport as a therapeutic target of cancer. *J. Hematol. Oncol.* **7,** 85 CrossRef Medline

64. Sun, Q., Chen, X., Zhou, Q., Burstein, E., Yang, S., and Jia, D. (2016) Inhibiting cancer cell hallmark features through nuclear export inhibition. *Signal Transduct. Target Ther.* **1,** 16010 CrossRef Medline

65. Saito, S., Cigdem, S., Okuwaki, M., and Nagata, K. (2016) Leukemia-associated Nup214 fusion proteins disturb the XPO1-mediated nuclear–cytoplasmic transport pathway and thereby the NF-κB signaling pathway. *Mol. Cell. Biol.* **36,** 1820–1835 CrossRef Medline

66. Sandén, C., Ageberg, M., Petersson, J., Lennartsson, A., and Gullberg, U. (2013) Forced expression of the DEK-NUP214 fusion protein promotes proliferation dependent on upregulation of mTOR. *BMC Cancer* **13,** 440 CrossRef Medline

67. Westerfield, M. (1995) *The Zebrafish Book: A Guide for the Laboratory Use of Zebrafish (Danio rerio)*, University of Oregon Press, Eugene, OR

68. Kimmel, C. B., Ballard, W. W., Kimmel, S. R., Ullmann, B., and Schilling, T. F. (1995) Stages of embryonic development of the zebrafish. *Dev. Dyn.* **203,** 253–310 CrossRef Medline

69. Yan, Y. L., Hatta, K., Riggleman, B., and Postlethwait, J. H. (1995) Expression of a type II collagen gene in the zebrafish embryonic axis. *Dev. Dyn.* **203,** 363–376 CrossRef Medline

70. Perner, B., Englert, C., and Bollig, F. (2007) The Wilms tumor genes wt1a and wt1b control different steps during formation of the zebrafish pronephros. *Dev. Biol.* **309,** 87–96 CrossRef Medline

71. Leimeister, C., Bach, A., and Gessler, M. (1998) Developmental expression patterns of mouse sFRP genes encoding members of the secreted frizzled related protein family. *Mech. Dev.* **75,** 29–42 CrossRef Medline